

**This item is the archived peer-reviewed author-version of:**

Applications of photoredox catalysis for the radical-induced cleavage of C-C bonds

**Reference:**

Vanderghinste Jaro, Das Shoubhik.- Applications of photoredox catalysis for the radical-induced cleavage of C-C bonds  
Synthesis : journal of synthetic organic chemistry - ISSN 1437-210X - 54:15(2022), p. 3383-3398  
Full text (Publisher's DOI): <https://doi.org/10.1055/A-1702-6193>  
To cite this reference: <https://hdl.handle.net/10067/1894720151162165141>

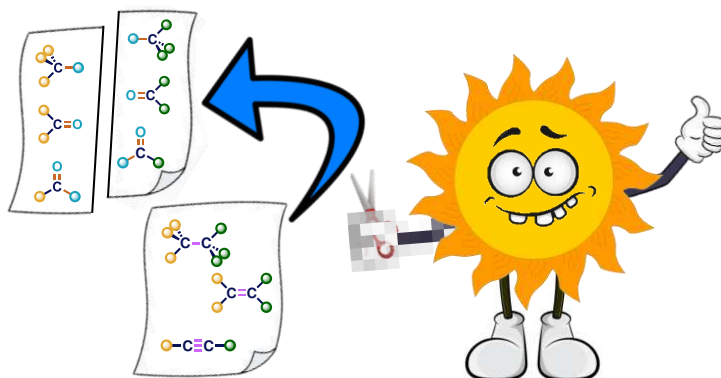
---

# Applications of Photoredox Catalysis for the Radical-Induced Cleavage of C-C Bonds

J. Vanderghinste  
S. Das\*<sup>a</sup>

<sup>a</sup> Organic Synthesis Division, Department of Chemistry,  
University of Antwerp  
Groenenborgerlaan 171, 2020 Antwerp (Belgium)

Shoubhik.Das@uantwerpen.be



**Abstract** Selective cleavage of C–C bonds forms one of the greatest challenges in current organic chemistry, due to the relative strength of these bonds. However, such transformations are an invaluable instrument to break down and construct new carbon–carbon bonds. To achieve this, photochemistry can be used as a tool to generate radicals and induce the cleavage of these bonds due to their high reactivity. This review examines some of the most influential contributions in this field since 2010.

- 1 Introduction
- 2 C–C Bond Cleavage
  - 2.1 Homogeneous Catalyst
    - 2.1.1 N-Centered Radical
    - 2.1.2 O-Centered Radical
  - 2.2 Heterogeneous Catalyst
- 3 C=C Bond Cleavage
  - 3.1 Homogeneous Catalyst
  - 3.2 Heterogeneous Catalyst
- 4 C≡C Bond Cleavage
  - 4.1 Homogeneous Catalyst
  - 4.2 Heterogeneous Catalyst
- 5 Conclusion

**Key words** photochemistry, radicals, C–C bond cleavage, visible light, homogeneous, heterogeneous

## Introduction

Second to hydrogen, carbon is the most abundant element present in organic structures which is reflected by the fact that such molecules largely consist of carbon-carbon bonds. Unfortunately, due to their covalent and unpolarised nature, cleavage of these bonds has proven to be challenging. Therefore, over the last few decades, much effort has been put into the development of new procedures to achieve this transformation.<sup>1</sup>

Traditionally, similar to activation of C-H bonds, it was proposed to activate C-C bonds via the insertion of a transition metal.<sup>2</sup> Thermodynamically, however, M-H bonds are generally stronger than M-C bonds.<sup>3</sup> Therefore, one can easily see that the activation of a

---

C-C bond via metal insertion is only thermodynamically feasible when the bond dissociation energy (BDE) of two M-C bonds exceeds that of the C-C bond. One way to manage this, is to select the metal catalyst based on the M-C bond strength. For example, M-C<sub>aryl</sub> bonds are relatively strong in the cases of Rh and Ir, sometimes even stronger than M-H bonds.<sup>4</sup> Another way to facilitate the metal insertion is to introduce strain in the substrate, hereby allowing for strain relief in the product and transition state as a kinetic and thermodynamic driving force in the C-C activation via metal insertion.<sup>5</sup> For unstrained C-C bonds, methods such as chelation assistance and decarbonylation can also be used.<sup>6</sup>

Besides the activation via metal insertion, another powerful tool for the C-C bond cleavage was found in radical chemistry, which has seen major developments over the years.<sup>7</sup> An attractive method to access these reactive radical species is via photoredox chemistry, where light irradiation is used as the energy source to trigger single electron transfer (SET) processes.<sup>8</sup> Because photoredox chemistry allows for a remarkable selectivity and functional group tolerance under mild reaction conditions, it sparks an enormous attraction in the organic chemistry community as the increasing need for sustainable approaches increases.<sup>9</sup>

This mini-review focuses on the application of photoredox chemistry towards the cleavage of carbon-carbon single, double and triple bonds, with the emphasis on providing a broad overview on recent literature reports, more so than on the fundamental theory behind the chemical transformation. To our knowledge, there have not yet been any similar reports where all three types of carbon-carbon bonds are discussed. Reports discussed in this perspective are categorized based on the type of catalyst and in one case, further classification was performed with the aim of maintaining a clear overview.

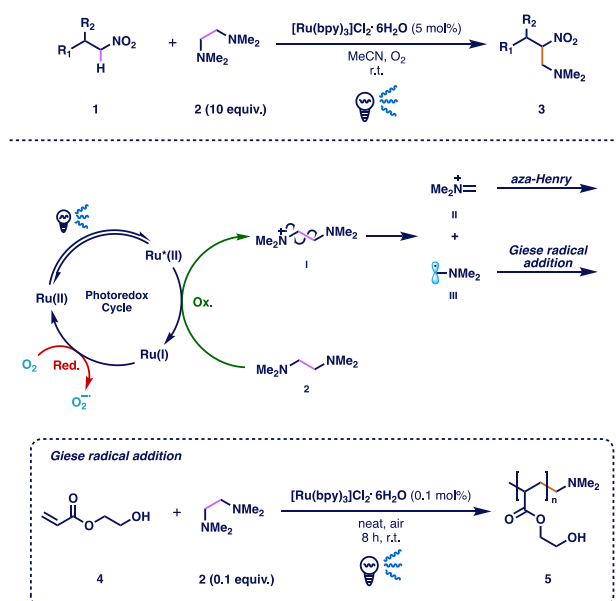
## C-C bond cleavage

The C-C single bond is evidently more challenging to undergo cleavage than the double or triple bonds, due to the lack of  $\pi$ -electrons. Therefore, such cleavage reactions are currently only available for activated C-C bonds, with an adjacent heteroatom. This results in the majority of the procedures utilizing a heteroatom radical to initiate a  $\beta$ -scission.

### Homogeneous catalyst

#### *N*-centered radical

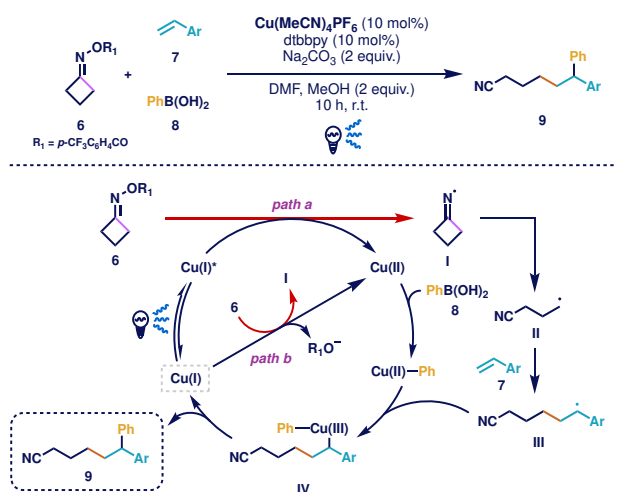
One of the first procedures for the photocatalytic cleavage of C-C single bonds was published in 2012 by the Wang group (**Scheme 1**).<sup>10</sup> They managed to generate two reactive species, namely an iminium ion **II** and  $\alpha$ -amino radical **III**, via the single-electron oxidation of *N,N,N',N'*-tetramethylethylenediamine (TMEDA) **2** by a homogeneous ruthenium complex. Both species could engage in transformations individually, as depicted in **Scheme 1**. Upon excitation of the photocatalyst using visible light, the excited state readily oxidized the diamine substrate **2** through a single-electron transfer (SET) event, yielding the reduced Ru(I) photocatalyst, which was oxidized back to the active Ru(II) species by oxygen gas, and radical cation of TMEDA **I**. A reorganization of the electron density on this radical cation caused the cleavage of the central C-C single bond, providing the iminium ion **II** and  $\alpha$ -amino radical species **III**. The authors proved this concept by performing an aza-Henry reaction with the *in situ*-generated iminium ion **II** for 11 substrates, with yields ranging between 63% and 91%. Additionally, they performed a single reaction where olefin **4** underwent a polymerization after a Giese-type radical addition of  $\alpha$ -amino radical **III**.



**Scheme 1** Mechanism of Wang's ruthenium-catalyzed C-C bond cleavage of TMEDA.

In 2018, Xiao and co-workers successfully performed a copper-catalyzed three-component coupling involving oxime esters, styrenes, and boronic acids (**Scheme 2**).<sup>11</sup> In this case, the oxime ester **6** underwent SET by the copper catalyst, yielding the N-centered iminyl

radical intermediate **I** that initiated the opening of the strained cyclobutane ring (path a). The resulting  $\gamma$ -cyanoalkyl radical **II** could then undergo a coupling with the styrene substrate **7**, providing radical intermediate **III**, which then engaged in an oxidative addition to the  $\text{LCu}^{\text{II}}\text{Ph}$  species that was obtained via transmetalation of the boronic acid **8**. The coupled product was then obtained through rapid reductive elimination of the high-valent  $\text{Cu}(\text{III})$  complex. Remarkably, when performing the reaction in the dark, the yield only decreased from 72% to 50%, suggesting an alternative pathway in the mechanism that circumvents excitation of the copper(I) catalyst (path b).



**Scheme 2** Mechanism of Xiao's copper-catalyzed three-component coupling of oxime esters, boronic acids and styrenes.

A year later, Xiao published another three-component coupling of oxime ester, this time with carbon monoxide gas and amines.<sup>12</sup> In this mechanism, however, after the oxidative addition of the  $\gamma$ -cyanoalkyl radical to the copper center, CO-insertion occurs to provide the coupled amide product after reductive elimination.

Another application of oxime esters was described in 2019 by the Wu group, where the iminyl radical intermediate was formed to initiate a C-C bond cleavage that generated open-shell acyl radicals which were then captured by a variety of Michael acceptors such as styrenes or acrylamides.<sup>13</sup>

Previously, the  $\gamma$ -cyanoalkyl radical was preferably generated from oxime esters over oximes to avoid competitive O-H bond dissociation.<sup>14</sup> However, the Yang group was able to generate the key iminyl radical intermediate via scission of the oxime N-O bond.<sup>15</sup> The excited  $\text{Ir}(\text{III})$  catalyst ( $E_{1/2} = +1.21$  V vs. SCE)<sup>16</sup> was reductively quenched by  $\text{PPh}_3$  ( $E_{1/2} = +0.98$  V vs. SCE)<sup>17</sup> to obtain  $\text{Ir}(\text{II})$  and the triphenylphosphine radical cation. In the presence of base, a new O-P bond could be formed with the oxime which readily underwent  $\beta$ -scission to generate the key iminyl radical. A sequential ring-opening through C-C bond cleavage provided the open-shell  $\gamma$ -cyanoalkyl radical that was captured by alkenes to generate a C-centered radical species. After reductive SET by the  $\text{Ir}(\text{II})$  catalyst, a reduced anionic intermediate was formed which readily abstracted a proton or attacked an electrophile.

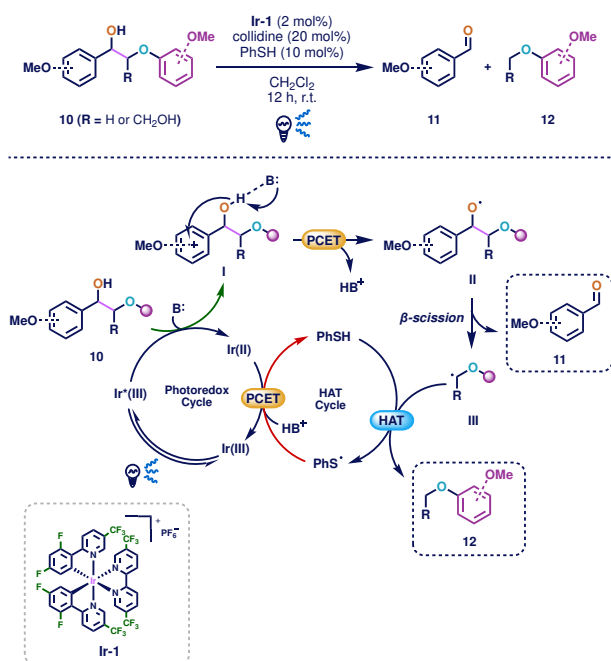
#### O-centered radical

In 2013, the Xia group described a procedure for the oxidative  $\text{C}_\alpha\text{-C}_\beta$  single bond cleavage of aldehydes under visible light.<sup>18</sup> Here, the aldehyde reacted with piperidine to form an enamine *in situ*, which could consecutively undergo a single-electron oxidation by the excited ruthenium(II) photocatalyst. This yielded the reduced ruthenium(I) photocatalyst, which could be converted to the active ruthenium(II) species via reductive quenching by molecular oxygen. On the other hand, upon reaction with a superoxide radical, the oxidized enamine radical intermediate formed a cyclic dioxetane species which delivered the product through expulsion of *N*-formyl piperidine. Via this pathway, Xia et al. developed a tandem reaction where the oxidative C-C bond cleavage was preceded by an intramolecular Michael addition. Here, piperidine was replaced by diisopropyl amine (DIPA) which, besides yielding the reactive enamine species in the second step, also served as a catalyst in the Michael addition.

The Soo group was, in 2015, one of the first to design a procedure for the visible-light-mediated C-C bond cleavage of lignin, and hereby paved the way for others to follow.<sup>19</sup> Prior protocols primarily involved cleavage of the C-O ether bond using expensive Ir-based photosensitizers and sacrificial reducing agents.<sup>20</sup> Soo, on the other hand, was able to selectively cleave the C-C bond using an earth-abundant vanadium (V) oxo complex. In 2017, the same group performed kinetic and density functional theory (DFT) studies where they investigated other vanadium(V) oxo complexes for their potential in the lignin C-C bond cleavage and successfully uncovered other catalysts that lowered the activation energy barrier and increased selectivity.<sup>21</sup> Despite the procedure being selective towards C-C bonds over C-O bonds, it appeared that multiple C-C bonds could be targeted as various fragments in yields ranging from 6% to 70% were observed after the reaction.

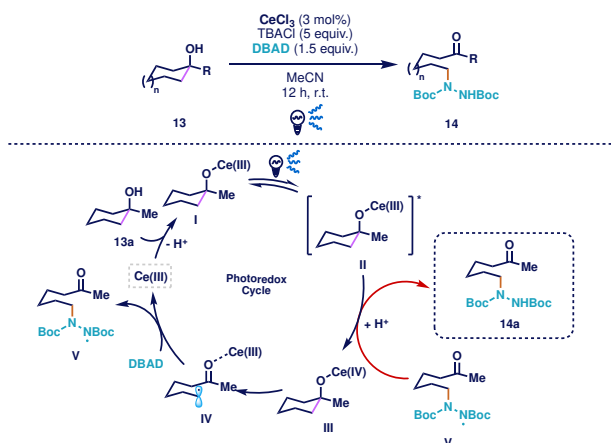
Trying to improve this selectivity, the Zhang group successfully developed a highly selective  $\text{C}_\alpha\text{-C}_\beta$  cleavage of lignin model substrates using an  $\text{Ir}(\text{III})$  catalyst **Ir-1** (Scheme 3).<sup>22</sup> The mechanism involved SET from the aromatic moiety of the substrate to the excited  $\text{Ir}(\text{III})$  catalyst, providing the radical cation intermediate **I**. Presence of a base allowed for a PCET event that caused relocation of the free electron towards the alkoxy oxygen atom. Radical species **II** was key in C-C cleavage reactions, as it could initiate a  $\beta$ -scission, a powerful tool to selective bond cleavage. After the  $\beta$ -scission, C-centered anisole radical **III** was generated which was quenched by thiophenol

through a HAT event. The high selectivity of the reaction was reflected in the fact that they obtained the aldehyde **11** and anisole **12** fragments in yields of up to 97 and 96% respectively.



**Scheme 3** Mechanism of Zhang's iridium-catalyzed C-C bond cleavage of lignin model substrates.

In 2016, Zuo and his team described the C-C bond  $\beta$ -scission of cyclic alcohols, generating a radical species that was trapped by di-*tert*-butyl azodicarboxylate (DBAD) under visible light (**Scheme 4**).<sup>23</sup> Under visible light, the cerium chloride/alcohol complex **I** was brought to its strongly reducing excited state **II** ( $E_{1/2} = -2.2 \text{ V vs. SCE}$ ), readily reducing nitrogen-centered radical intermediate **V** which generated Ce(IV) species **III**. The authors believed that the following  $\beta$ -scission was facilitated due to the oxidizing nature of Ce(IV) species **III**. This generated a reactive radical intermediate **IV** that promptly coupled with DBAD to generate the nitrogen-centered radical intermediate **V**, which was reduced by the excited Ce(III)/alcohol complex **II** to provide the product **14**.

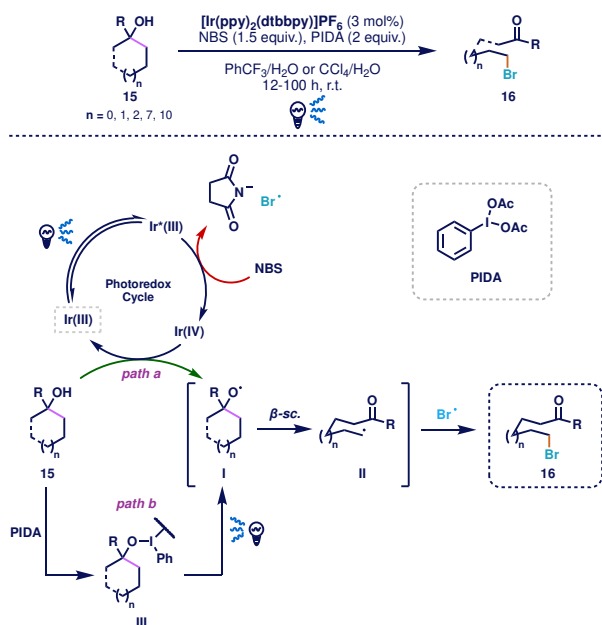


**Scheme 4** Mechanism of Zuo's cerium-catalyzed C-C bond cleavage of cyclic alcohols.

The Knowles group successfully eliminated the need for the DBAD radical trap by introducing thiophenol to trigger a HAT event that would quench the carbon-centered radical.<sup>24</sup> Another adjustment they made was replacing CeCl<sub>3</sub> by an Ir(III) complex (**Ir-1**).

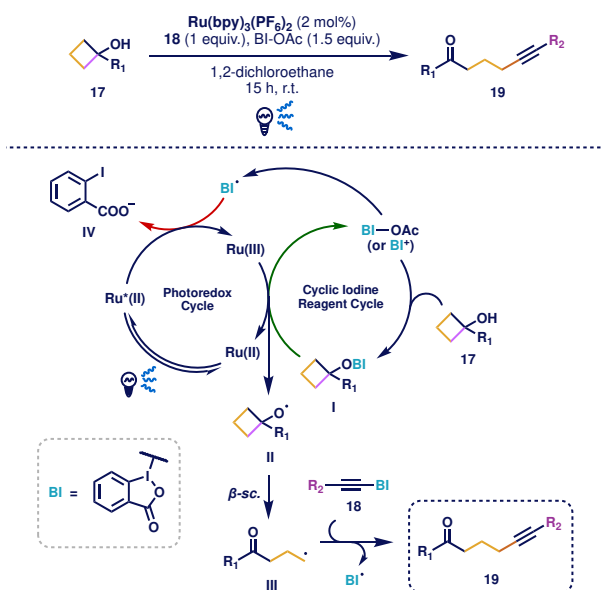
A major limitation of this reaction, however was that a strongly electron-donating *p*-methoxyphenyl (PMP) substituent on the  $\alpha$ -carbon atom was mandatory to successfully yield the reaction product. The excited photocatalyst initiated the reaction by abstracting an electron from the PMP unit, which, in the presence of a base, accepted an electron from the proximal oxygen atom, yielding the corresponding alkoxy radical. Consecutive  $\beta$ -scission and HAT then delivered the desired ketone product while thiophenol was regenerated via an electron transfer from the Ir(II) species followed by a proton transfer from the protonated base. They later improved the reaction conditions as the need for the strongly electron-donating PMP substituent was avoided by selecting a different Brønsted base and HAT reagent.<sup>25</sup>

Instead of trapping the radical with a hydrogen atom as in Knowles' reaction, Zhu showed in 2018 that adding *N*-bromosuccinimide (NBS) could deliver the brominated product (**Scheme 5**).<sup>26</sup> Besides the conventional PCET mechanism in which the photocatalyst provided the alkoxy radical **I** (path a), an alternative pathway was proposed. Here, the key alkoxy radical intermediate **I** was obtained through visible-light-mediated homolytic cleavage of the oxygen-iodine bond in the alcohol-PIDA construction **III** (path b). However, both pathways involved visible light, as performing the reaction in the dark provided no product.



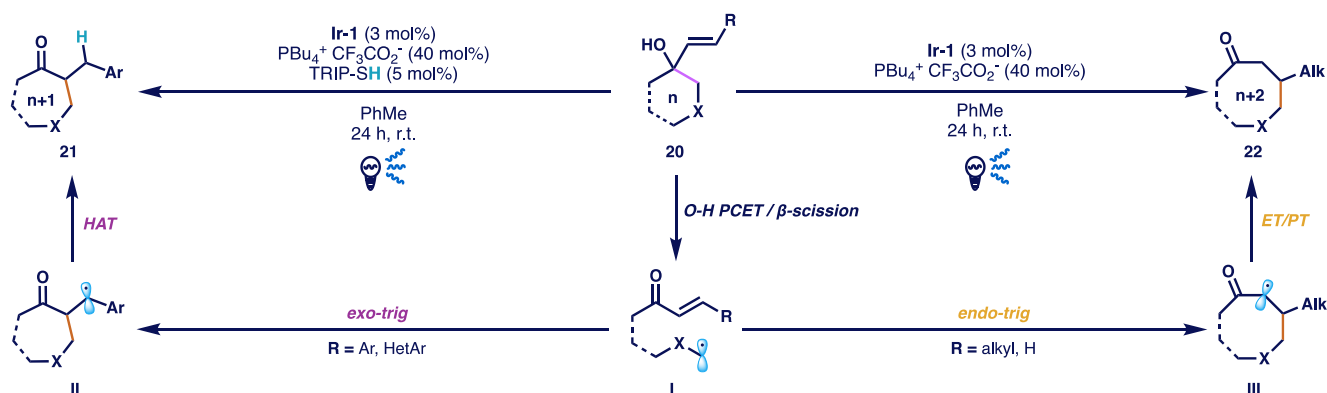
**Scheme 5** Mechanism of Zhu's iridium-catalyzed C-C bond cleavage of cyclic alcohols.

The use of hypervalent iodine reagents for the  $\beta$ -C-C cleavage of alcohols was inspired by the work of Chen and co-workers, who performed their reaction using a ruthenium(II) photocatalyst in the presence of a cyclic iodine(III) reagent (**Scheme 6**).<sup>27</sup> Acetylbenziodoxole (BI-OAc) readily generated BI<sup>+</sup> ions that served as a Lewis acid to coordinate with the alcoholic oxygen atom to give intermediate **I**. Homolytic cleavage of this newly formed I-O bond was facilitated via SET by the oxidized ruthenium species, initiating the  $\beta$ -scission that yielded the C-centered alkyl radical **III** which then underwent radical addition to the alkynyl-bound benziodoxole **18**. The procedure proved successful for both strained cyclic as well as linear alcohols and was the first visible-light-mediated alcohol oxidation to generate alkoxy radicals using a cyclic iodine(III) catalyst. However, a minor setback of this procedure was the requirement of pre-formed alkynyl-BI instead of forming it *in situ*.



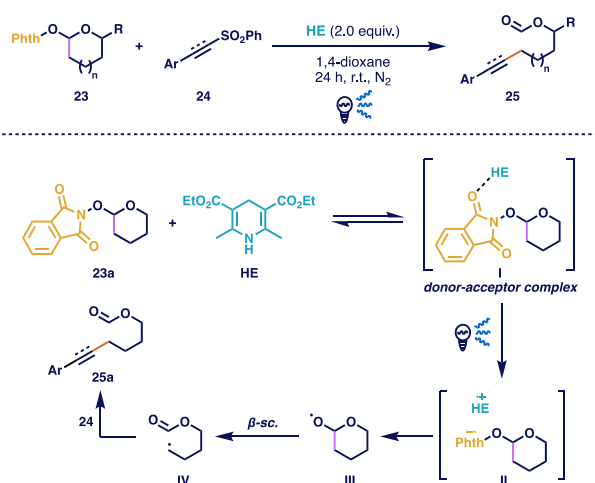
**Scheme 6** Mechanism of Chen's ruthenium-catalyzed C-C bond cleavage of strained cyclic and linear alcohols.

Another procedure that made use of the alkoxy radical intermediate was the catalytic ring expansion of cyclic alcohols described by the Knowles group (**Scheme 7**).<sup>28</sup> In this context, PCET activation of the O-H bond by a Brønsted base and an excited Ir(III) catalyst allowed for the formation of the key alkoxy radical species, which then mediated the  $\beta$ -scission of an adjacent C-C bond to deliver a new carbonyl group and a terminal C-centered radical **I**. This radical was then trapped by introducing an olefinic moiety on the alcoholic carbon atom of the substrate **20**, authorizing either an n+1- or n+2-sized ring in an exo- or endo-trig event, respectively.



**Scheme 7** Mechanism of Knowles' iridium-catalyzed ring-expansion via C-C bond cleavage of cyclic alcohols.

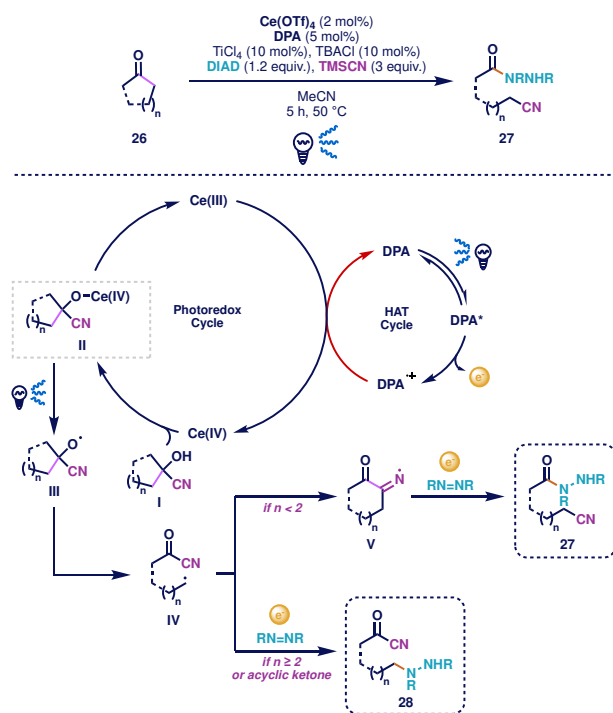
Wang described photoinduced ring-opening of cyclic hemiacetals through  $\beta$ -scission of alkoxy radicals with Hantzsch ester (HE) as the reductant (**Scheme 8**).<sup>29</sup> Upon activation of the hemiacetal with *N*-hydroxyphthalimide (NHPI), coordination with HE resulted in a donor-acceptor complex **I** that allowed for SET reduction of the substrate upon visible-light irradiation. After elimination of the phthalimido moiety, alkoxy radical **III** was generated which initiated the crucial  $\beta$ -scission, providing C-centered radical **IV** that could be trapped by alkynyl sulfones **24** to obtain the alkynylated product **25**. Additionally, alkenyl sulfones were introduced as radical trap and provided the alkenylated products in moderate yields ranging between 54% and 78%. It has to be noted that HE was required in stoichiometric amounts, therefore, this reaction was not of a catalytic nature.



**Scheme 8** Mechanism of Wang's Hantzsch ester-mediated C-C bond cleavage of hemiacetals.

In 2020, the Zuo group described the C-C bond cleavage of both cyclic and acyclic ketones via generation of the alkoxy radical using a cerium(IV) catalyst (**Scheme 9**).<sup>30</sup> The addition of  $\text{TiCl}_4$  as Lewis acid and  $\text{TMSCN}$  to the ketone substrate delivered the corresponding cyanohydrin **I** which was then prone for subsequent coordination with the cerium catalyst and visible-light-mediated Ce-O bond cleavage to yield the O-centered radical species **III**. Following  $\beta$ -scission led to a distal carbon-centered radical **IV** for which the consecutive reaction pathway depended on the ring size of the substrate. For cyclobutanones or -pentanones ( $n < 2$ ), the alkyl radical underwent an addition to the nitrile carbon atom, generating the iminyl intermediate **V** which readily mediated a cleavage of the adjacent C-C bond, causing a net migration of the cyanide group to form the product **27**. For 6-membered, or larger, rings and acyclic ketones, the alkyl radical **IV** was trapped by diisopropyl zodiacarboxylate (DIAD), avoiding migration of the CN-moiety.

In 2021, Knowles and co-workers were convinced that the alkoxy radical could be generated from hydroxyl substituents in commercial phenoxy resin and high molecular weight hydroxylated polyolefin derivatives in order to cleave the adjacent C-C bond and cause polymer degradation.<sup>31</sup> The requirement of photocatalyst, base and a thiol indicated the presence of a consecutive PCET/ $\beta$ -scission. However, the Knowles group did not perform detailed mechanistic studies to propose a reaction mechanism.



**Scheme 9** Mechanism of Zuo's dual-catalyzed C-C bond cleavage of cyclic alcohols.

After the reports in 2016 and 2020 on the Ce-mediated photocatalytic C-C bond cleavage, the Zuo group further expanded the application potential of cerium salts for this type of reaction (**Scheme 10**).<sup>32</sup> In this case, they performed a ring expansion via subsequent  $\beta$ -scission and oxidation of cyclic ketones. Whereas, in 2020, DPA was used to complete the cerium catalytic cycle, they now introduced cyanoanthracene as organic photocatalyst (OPC) as it apparently enhanced the turnover number (TON), rendering the target macrolactone product **30** within 20 minutes. Due to the Lewis acidic nature of Ce(III), the ketone/lactol equilibrium of **29a** shifted towards the lactol upon coordination with the metal salt. The *in situ*-formed cerium(III) lactol complex ( $E_{1/2} = 0.40$  V vs. SCE) would be readily oxidized by the radical cation of cyanoanthracene ( $E_{1/2} = 1.61$  V vs. SCE), to the Ce(IV) state, which provided alkoxy radical **I** upon photoirradiation through Ce-O bond cleavage. After the  $\beta$ -scission, C-centered radical **II** was generated that captured  $\text{O}_2$ , delivering peroxy radical **III** that, after subsequent reduction and protonation was converted to the product **30a** after releasing  $\text{H}_2\text{O}$ .

The tolerability of Zuo's procedure towards a broad range of substrates was proven, as over 55 diverse substrates, were converted to their respective macrolactone products with ring-sizes of up to 19. Additionally, the procedure was successfully applied to the concise synthesis of sonnerlactone, metabolite hat was isolated from fungi found in the South China Sea.<sup>33</sup>

A recent report by the Mo group, involved a novel procedure for the photo-induced radical borylation of hemiacetal derivatives via the C-C bond cleavage.<sup>34</sup> Their method provided a facile new synthetic route for boronic esters as invaluable reagents in, for example, cross-coupling reactions.<sup>35</sup> DFT calculations confirmed the proposed mechanism, which was initiated when the substituted hemiacetal substrate **23** interacted with solvated bis-catecholato)diboron ( $\text{B}_2(\text{cat})_2$ ) to form an additive that could be activated through energy transfer by  $\text{Ir}(\text{ppy})_3$ . This photosensitizing process generated a radical species that generated a O-centered hemiacetal radical intermediate to promote ring-opening by  $\beta$ -scission. The obtained C-centered radical then added onto a boron atom in the solvated  $\text{B}_2(\text{cat})_2$  structure, which then underwent a B-B bond cleavage to deliver the final boronic ester product. Besides, 5-, 6-, and 7-membered rings, also linear hemiacetals were successfully borylated in yields of up to 81%.

## Heterogeneous catalyst

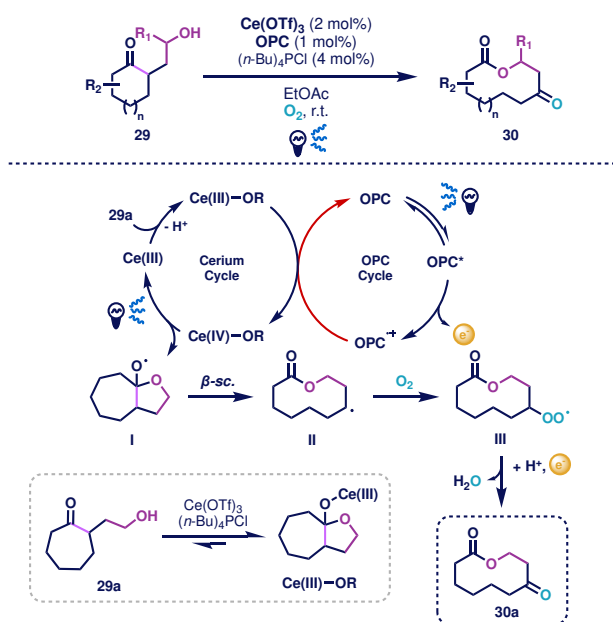
Heterogeneous catalysts have been used for quite a long time in the photocatalytic cleavage of carbon-carbon bonds, with reports dating back to 1996.<sup>36</sup> However, the majority of these reports are focused on the degradation of organic dyes, instead of applications in chemical synthesis.<sup>37</sup> As of today, the use of semiconductors in the selective C-C bond cleavage is still an enormous hurdle to cross.

In 2017, Yang and co-workers investigated the photocatalytic C-C bond cleavage in ethylene glycol (EG) on  $\text{TiO}_2$  and hereby studied the effect of deposited metal nanoparticles (NPs).<sup>38</sup> They revealed that pristine  $\text{TiO}_2$  was highly capable of converting EG to 2 equivalents of formaldehyde and hydrogen gas since the substrate molecules adsorbed purely on the Ti sites, not on the metal. However, introducing Pt, Pd, or Au NPs appeared to improve hydrogen desorption, which increased formaldehyde formation with Pt performing best. Since oxygen played a major role in the C-C bond cleavage, the risk of overoxidation of the aldehyde product towards  $\text{CO}_2$  gas was imminent. Also, the presence of water allowed for polymerization of the product, causing the formation of paraformaldehyde. In 2018, the same group probed for a relation between selectivity and the type of noble metal NPs.<sup>39</sup> They showed that Ag and Au promoted the formation of the polymer and suppressed overoxidation by rapidly providing water as adsorbed hydrogen atoms efficiently reacted with



superoxide radicals ( $O_2^{\cdot-}$ ). On the other hand, Pt promoted complete oxidation and inhibited polymerization due to the insufficient amount of water caused by an indirect pathway for water formation.

The Wang group published a report on the C-C bond cleavage in lignin models in 2018, using carbon nitrides under visible light.<sup>40</sup> In this study, three different catalysts were used: a carbon nitride material synthesized from melamine ( $C_3N_4$ -M), one from urea ( $C_3N_4$ -U), and one mesoporous graphitic carbon nitride (mpg- $C_3N_4$ ). The objective was to selectively perform the aerobic cleavage over the oxidation of the alcohol. Out of the three carbon nitride catalysts, mpg- $C_3N_4$  obtained the highest conversion (96%), together with the optimal selectivity towards the C-C bond cleavage (91%). Brunauer-Emmett-Teller measurements of the catalysts then revealed the significant structural difference between the three as the specific surface area for  $C_3N_4$ -M and  $C_3N_4$ -U were  $6.6 \text{ m}^2 \text{ g}^{-1}$  and  $48.2 \text{ m}^2 \text{ g}^{-1}$ , respectively, whereas mpg- $C_3N_4$  has a surface area of  $206.5 \text{ m}^2 \text{ g}^{-1}$ , explaining the increased catalytic activity of the latter. A similar trend could be observed for the pore volumes, where the values of  $C_3N_4$ -M,  $C_3N_4$ -U, and mpg- $C_3N_4$  were determined to be  $0.04 \text{ cm}^3 \text{ g}^{-1}$ ,  $0.15 \text{ cm}^3 \text{ g}^{-1}$ , and  $0.42 \text{ cm}^3 \text{ g}^{-1}$ . The authors proposed that after excitation of the semiconductor, a  $\beta$ -H of the substrate was abstracted at the valence band holes to generate a C-centered radical, which then captured oxygen gas to form the peroxy radical. The hydroperoxide intermediate formed after HAT, underwent a rearrangement through a 6-membered transition state to provide both cleavage products by releasing water. Finally, the reaction procedure was applied to 5 substrates, other than the model one, and even though high conversions were achieved (>88%), the selectivity of the C-C bond cleavage towards other scaffolds was not achieved.



**Scheme 10** Mechanism of Zuo's dual-catalyzed synthesis of macrolactones via C-C bond cleavage of cyclic ketones.

## C=C bond cleavage

Carbon-carbon double bonds are among the most common functional groups present in organic scaffolds and have also exhibited highly versatile applications in the synthesis of organic molecules through transformations such as addition,<sup>41</sup> cycloaddition,<sup>42</sup> metathesis,<sup>43</sup> reduction,<sup>44</sup> oxidation,<sup>45</sup> and polymerization.<sup>46</sup> Among these reactions, the oxidation of C=C bonds is a remarkable tool to obtain carbonyl-containing compounds such as aldehydes, ketones, carboxylic acids, esters, and amides. Traditional alkene oxidation reactions such as ozonolysis<sup>47</sup> and the Lemieux-Johnson oxidation<sup>48</sup> lack selectivity as well require harmful oxidants.

On the contrary, photocatalysis can provide a solution due to its potential to generate reactive oxygen species (ROS) such as singlet oxygen ( $^1O_2$ ) and  $O_2^{\cdot-}$ .<sup>49</sup> These species can undergo [2+2] cycloadditions with olefins or couplings with oxidized olefins, respectively, to provide a key dioxetane intermediate. This 4-membered ring can then undergo oxidative cleavage to generate two oxidized products containing a carbonyl moiety. As will become clear, most of the procedures discussed in this chapter will strongly rely on the formation of this cyclic intermediate.

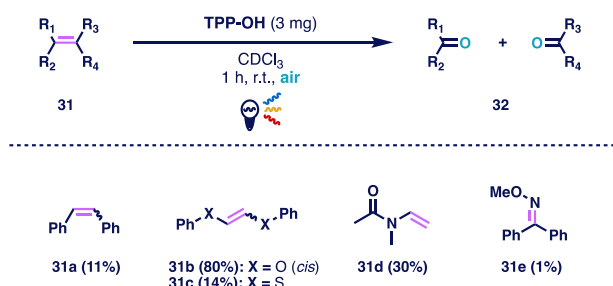
## Homogeneous catalyst

An early report of a photocatalytic C=C bond cleavage using a homogeneous catalyst was the work by Itoh and co-workers in 2009.<sup>50</sup> Here, a variety of styrenes successfully underwent an aerobic photo-oxidation to obtain the respective carboxylic acid. Prior to this work, the Itoh group had already studied these types of reactions using FSM-16, a mesoporous silica, and  $I_2$ .<sup>51</sup> However, this procedure proved inadequate when using  $\alpha$ - or  $\beta$ -substituted styrenes as the substrates. During a follow-up study, they discovered the cleavage of C=C bonds occurred in the presence of catalytic  $CBr_4$ . Under irradiation of an Hg lamp, one of the C-Br bonds of the catalyst was homolytically cleaved, generating reactive bromine radicals that readily added onto the double bond of the substrate. The resulting C-centered radical species then bonded with oxygen gas, after which hydrogen abstraction of a solvent molecule provided the hydroperoxide species. Upon

elimination of water, the  $\alpha$ -bromo ketone was formed, which, according to the authors, followed one of two reaction pathways, both delivering the acyl radical. The first possibility was that the radical was formed through a light-induced homolytic C-C bond cleavage. The second route started by generating a reactive bromine radical after cleavage of the C-Br bond of the substrate. The simultaneously generated, C-centered radical, reacted with oxygen to deliver the corresponding  $\alpha$ -hydroperoxy ketone. Subsequent elimination of water then provided the dione which underwent a C-C bond cleavage under UV-light irradiation, generating 2 equivalents of acyl radical. Addition of oxygen gas and hydrogen abstraction from the solvent then delivered the peroxy acid which was efficiently converted to the carboxylic acid under light irradiation. The substrate scope of the reaction showed that electron-deficient alkenes were not very well tolerated (4-nitrostyrene: 16% yield). This was expected since the C-centered radical that was formed upon the addition of Br $\cdot$ , is strongly destabilized by electron-withdrawing moieties, hereby preferring the unpaired electron to be on the adjacent carbon atom.

Five years later, Itoh published another, similar procedure which focused on the photooxidative C=C bond cleavage of stilbenes using I $_2$  and trifluoroacetic acid (TFA) instead of CBr $_4$  for radical generation.<sup>52</sup> Here, however, they proposed a mechanism slightly different from that in their work on the CBr $_4$ -mediated C=C bond cleavage.<sup>50</sup> In their most recent publication, an iodide and O-centered methoxy radical added onto the double bond, after which the C-I bond was cleaved under the irradiation of light, generating a C-centered radical intermediate. Subsequent reaction with oxygen gas and hydrogen abstraction provided the  $\alpha$ -methoxyhydroperoxide. Cleavage of the C-C bond was then allowed by elimination of water under acidic conditions, delivering the aldehyde and methyl oxonium salt. The latter could then be converted to the aldehyde product in the presence of methanol and acid.

In 2009, You and co-workers focused on the use of singlet oxygen, more specifically its [2+2] cycloaddition reaction, for the photochemical triggering of drug delivery systems such as liposomes or prodrugs (**Scheme 11**).<sup>53</sup> Since UV-light cannot penetrate deeper than 1 mm into tissue, only low energy light from the (near-)IR region can be used. For this, the authors selected 5,10,15-triphenyl-20-(4-hydroxyphenyl)-21*H*,23*H*-porphyrin (TPP-OH) as a photosensitizer. Without TPP-OH, nearly all substrates demonstrated negligible reactivity (<1%) with atmospheric oxygen and light irradiation. Unfortunately, only 4 out of 15 substrates exceeded a yield of 75%. One example was a dithiofunctionalized olefin **31c** which only delivered the carbonylated product in 14%. According to the authors, when comparing the 1,2-dioxy olefin **31b** (80%) with its thiolated counterpart **31c** (14%), the latter reaction was disadvantageous since more side products were being formed. However, despite the unfavorable reaction yields, a major advantage of this reaction that visible light of up to 800 nm could be used to successfully perform this C=C bond cleavage.



**Scheme 11** Part of the olefin scope of You's photosensitized, oxidative [2+2] cycloaddition.

In 2014, the Yadav group disclosed a procedure to oxidatively cleave C=C bonds through generation of O $_2^{\cdot-}$  with eosin Y as a homogeneous photocatalyst.<sup>54</sup> In this work, the excited photocatalyst was able to oxidize the styrene substrate to the radical cation intermediate, after which the reduction of O $_2$  to O $_2^{\cdot-}$  closed the catalytic circle and delivered the eosin Y back in its initial state. Later, radical-radical coupling generated the dioxetane intermediate, which underwent a cleavage reaction to deliver the aldehyde product upon releasing formaldehyde.

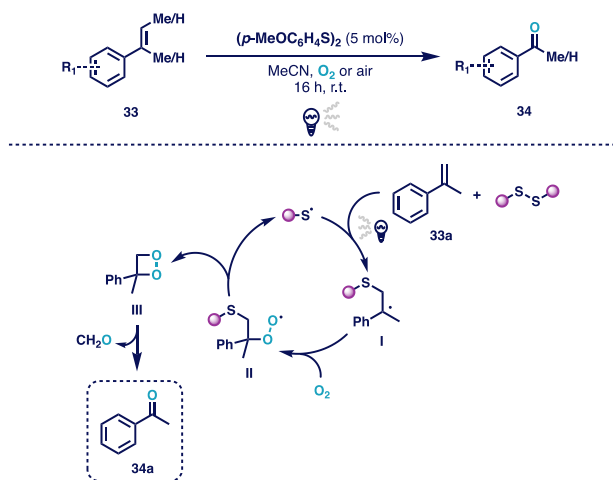
In the same year, Wang and co-workers published their procedure for the visible-light-induced photocatalytic conversion of enamines to amides.<sup>55</sup> In the presence of a Ru(II) complex, Cs $_2$ CO $_3$ , and oxygen gas, several enamine substrates were successfully converted to their formamide counterparts in yields ranging from 40% to 89%. Additionally, Wang's reaction procedure also tolerated ketone-derived enamines, as the corresponding amides were obtained in yields between 82 and 99%. However, this substrate scope was limited and only consisted of 4 enamines.

Continuing on enamines and their derivatives, the Lee group was able to convert the C=C bond in *N*-sulfonyl enamides to a C=O bond, contributing to the challenging selective acylation of azulenes.<sup>56</sup> Traditionally, harmful reagents such as POCl $_3$  (Vilsmeier-Haack)<sup>57</sup> or AlCl $_3$  (Friedel-Crafts)<sup>58</sup> were required, adding to the low yields, diacylation and poor functional group tolerance these reactions suffered from.<sup>59</sup> In Lee's work, they reported a synthetic procedure for azulene-1-yl ketones via oxidative cleavage of the C=C bond in *N*-sulfonyl enamides via the reaction with Cs $_2$ CO $_3$ , under air and sunlight and in the absence of a photosensitizer. Based on literature reports and experimental observations, the authors proposed a mechanism that was based on the formation of a dioxetane intermediate which was formed through a cyclization with oxygen.<sup>60</sup> This was suggested after labelling experiments with  $^{18}\text{O}_2$  delivered the  $^{18}\text{O}$ -inserted ketone product, unlike the reaction with H $_2^{18}\text{O}$ . Moreover, the oxidative cleavage did not proceed in the absence of light, indicating that the sunlight was crucial for the reaction. Additionally, the authors unveiled the importance of the N-H proton in the amine moiety of the *N*-sulfonyl enamide, as the experiments revealed that a 3 $^\circ$ -amine moiety in the enamide did not yield the ketone product. The mechanism proposed by the authors involved the formation of an alkene radical cation and O $_2^{\cdot-}$  through photoinduced electron transfer of a contact

charge-transfer (CCT) complex between the enamide substrate and O<sub>2</sub>. After the cyclization reaction, providing the dioxetane cyclic intermediate, it decomposed into the ketone product after abstraction of the N-H proton in the *N*-sulfonyl enamide. Both substrates containing electron-rich or electron-deficient aromatic moieties were tolerated and obtained in yields ranging from 85% to 91%. Even *N*-mesyl enamides with thiophen-2-yl and cyclohexen-1-yl groups were successfully converted, providing the respective products in 88% and 76% yields. Additionally, the authors were able to generate the *N*-sulfonyl enamide in situ through a tandem Cu-catalyzed [3+2] cycloaddition, Rh-catalyzed arylation, photooxygenation, and ring-opening reaction in one pot under air and sunlight. This, however, will be elaborated on in detail further down this perspective.

Besides enamines, enamines were also proposed by Wen and co-workers in 2015 as substrates towards the visible-light-induced C=C bond cleavage.<sup>61</sup> Similar to enamines, the carbon-carbon double bond was replaced with C=O, hereby generating 1,2-diones instead of monoketones with enamines as substrates.

In 2017, Noël and Wang disclosed a visible-light-mediated oxidative cleavage of C=C bonds and hereby found evidence of an olefin-disulfide charge-transfer complex (Scheme 12).<sup>62</sup> Upon looking for a photoinitiated radical that could reversibly add to the C=C bond of the substrate, they imagined that thiyl radicals generated by the photolysis of disulfides could be ideal.<sup>63</sup> However, dissociation of typical aromatic S-S bonds cannot occur under visible light and therefore require UV irradiation.<sup>64</sup> Nevertheless, a study from 1951 performed by Mantell and co-workers revealed that the reaction rate of the radical addition of a thiyl radical to an olefin was significantly higher than the SET oxidation of thiol by itself, owing to the formation of an olefin-thiol charge-transfer complex (CTC).<sup>65</sup> The work done by Noël and Wang relied on this principle and hereby extended it towards disulfides, which had not been reported prior to this. The authors confirmed the presence of the CTC by looking at the upfield shift of the methoxy protons in bis(4-methoxyphenyl) disulfide in the presence of olefin. Higher olefin/disulfide ratios accounted for stronger upfield shifts, indicating an increasing electron density on the disulfide. They also performed control experiments where two different disulfide substrates were mixed under visible light, in the absence of olefin. Since, after 1h, no mixed disulfide had been formed, it could be concluded that the S-S bond cleavage did not occur under visible light in the absence of olefin. Performing the same reaction with irradiation from a medium-pressure Hg lamp did, in fact, provide 9% of the product. Regarding the mechanism, the thiyl radical formed through CTC-mediated photolysis of the S-S bond readily added onto the olefin **33**, generating a C-centered radical **I** that could capture molecular oxygen to form the peroxy radical intermediate **II**. Then, a cyclization reaction occurred, providing the dioxetane intermediate **III**, which decomposed to yield the ketone product **34**. All products were obtained in yields ranging from 60% to 92%, with the only exception being (*Z*)- $\beta$ -methylstyrene (44%), in which part of the starting material was either epoxidized or isomerized to the (*E*)-alkene.



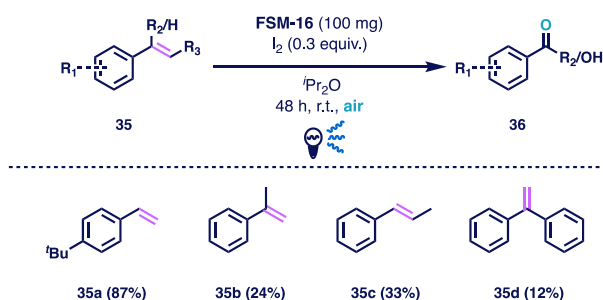
**Scheme 12** Mechanism of Noël and Wang's disulfide-catalyzed oxidative C=C bond cleavage of olefins.

The Wan group designed a novel synthesis route for  $\alpha$ -ketoesters via the aerobic C=C bond cleavage using a metal-free photocatalyst.<sup>66</sup> Here, rose bengal was excited under visible-light irradiation, after which the excited species activated oxygen gas to provide reactive singlet oxygen.<sup>67</sup> This species then coupled to the C=C bond of the enaminone substrate to generate the dioxetane intermediate which underwent a ring-opening reaction triggered by a protonation. Subsequent to the ring-opening reaction, a new N-O bond was formed to provide a 4-membered cyclic intermediate which provided a zwitterionic species upon nucleophilic attack of an alcohol. This species then decomposed into the  $\alpha$ -ketoester product and an amino alcohol. A broad substrate scope exhibited the tolerability of the reaction procedure towards various enaminone substrates as all products were obtained in yields between 65% and 84%. Additionally, the conversion of the natural 16-dehydropregnenolone acetate to its respective  $\alpha$ -ketoester was successful, achieving a yield of 45%.

### Heterogeneous Catalyst

In 2002, Inagaki and co-workers were able to synthesize carboxylic acids via the C=C bonds cleavage using I<sub>2</sub> and a mesoporous, recyclable silica (FSM-16) photocatalyst (Scheme 13).<sup>51</sup> However, their substrate scope proved the limited applicability of the reaction since substrates with di- (or higher) substituted double bonds (**35b-d**) were only converted in poor yields between 12% and 33%.

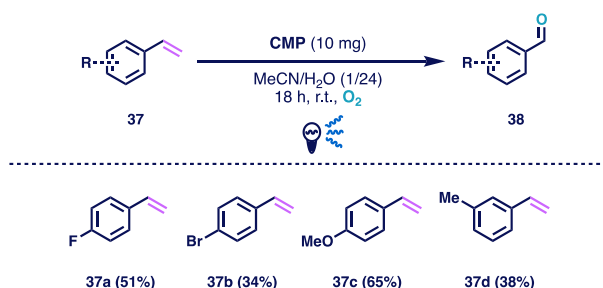
Furthermore, when submitting the aliphatic 1-dodecene to the reaction, no product formation was observed. However, this reaction provided sufficient foundation for further research by Itoh and others.<sup>50, 52, 68</sup>



**Scheme 13** Part of the olefin scope of Inagaki's silica-catalyzed oxidative C=C bond cleavage.

After the Hirai group noticed that silica-based materials showed promising results in the photocatalytic oxidation of olefins with oxygen, they compared a range of heterogeneous catalysts and published their results in 2006.<sup>69</sup> In previous reports, often photocatalytic systems based on TiO<sub>2</sub> were described, which were operative in the UV range and promoted complete oxidation of the olefins to CO<sub>2</sub>.<sup>70</sup> During their investigation, the authors' target was not the cleavage of C=C bonds, however, after the reaction, the cleaved product was observed. Among the assessed catalyst materials, Cr-SiO<sub>2</sub> prepared by a conventional sol-gel method provided the highest yield in the majority of the substrates, reaching up to 89% of the ketone product obtained via C=C bond cleavage. A major setback of this reaction was the limited substrate scope. Additionally, the procedure was only successful for terminal alkenes.

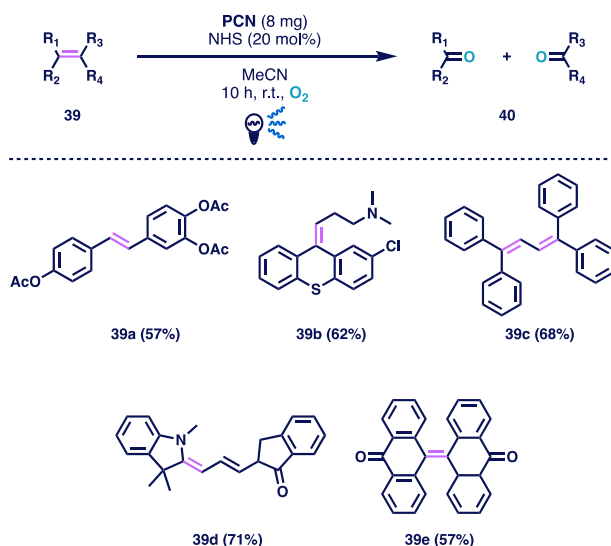
Instead of these inorganic heterogeneous photocatalysts, Zhang and co-workers performed their visible-light-promoted C=C bond cleavage of styrene with conjugated microporous polymers (CMPs) as photocatalysts (**Scheme 14**).<sup>71</sup> Three CMPs were compared, which were synthesized from triethynylbenzene and thiophene (BTh), triethynylbenzene and benzothiadiazole (BBT), and triethynylbenzene with 50% thiophene and 50% benzothiadiazole (BThBT). The authors selected these catalysts based on their different electron affinities, since the thiophene moiety act as a strong electron donor while the benzothiadiazole has strong electron-accepting properties. During the screening experiments, it became clear that the solvent polarity strongly influenced the benzaldehyde formation. Hence, the optimal solvent system was determined to be MeCN/H<sub>2</sub>O (V/V = 1/24). Among the catalysts, BBT performed best, achieving a conversion of 91% with 85% of benzaldehyde formed. This was in agreement with the pore volume measurements, where BBT had the highest volume of 0.631 cm<sup>3</sup> g<sup>-1</sup>. Counterintuitively, Brunauer-Emmett-Teller (BET) measurements showed that the BBT catalyst had the smallest surface area of only 129 m<sup>2</sup> g<sup>-1</sup> compared to BThBT with 445 m<sup>2</sup> g<sup>-1</sup> and BTh with 806 m<sup>2</sup> g<sup>-1</sup>. The authors also determined the band structures of all three catalysts and revealed that BBT exhibited the highest LUMO level at -0.92 V vs SCE, indicating its strong ability to generate O<sub>2</sub><sup>•-</sup> from O<sub>2</sub> for which a potential of only -0.57 V vs SCE is required. The formation of this intermediate was crucial in the proposed mechanism where, upon excitation with visible light, the substrate **37** was oxidized at the HOMO of the semiconductor, generating a radical cation intermediate. At the LUMO of the photocatalyst, superoxide radicals were generated through reduction of oxygen gas. This species then reacted with the styrene radical and delivered a dioxetane intermediate. 1-phenyl-1,2-ethanediol was then formed due to exposure to water, which was eventually cleaved into the aldehyde product **38**, releasing formaldehyde as potential side product. Overall, even though all substrates were almost completely converted (>99%), selectivity towards the cleavage reaction product was relatively low (27-65%) and in some cases, the aldehyde was not present.



**Scheme 14** Part of the styrene scope of Zhang's CMP-catalyzed oxidative C=C bond cleavage.

Staying in the field of polymeric catalysts, the Das group was able to cleave C=C bonds using polymeric carbon nitrides (PCN) to generate the key superoxide radical species.<sup>72</sup> These catalysts were able to initiate this SET reduction reaction, according to the position of the conduction band at -1.55 V vs. SCE.<sup>73</sup> After the optimization, the reaction conditions were set at 0.25 mmol of substrate, 8 mg of PCN catalyst, and 20 mol% of *N*-hydroxysuccinimide (NHS) in MeCN in an O<sub>2</sub> atmosphere and under irradiation of blue LED. Regarding the mechanism, two plausible mechanisms were proposed by Das et al.. Both were starting from the excitation of the semiconductor, which reduced O<sub>2</sub> to O<sub>2</sub><sup>•-</sup> at the conduction band while generating a radical cationic intermediate through oxidation of the substrate at the valence band. The first reaction pathway involved the traditional cyclization reaction between both radical species, hereby providing the dioxetane intermediate which underwent a ring-opening reaction to give the two cleavage products. The second pathway, however,

included the beneficial effect of NHS, whereas HAT from NHS to  $O_2^{\cdot-}$  delivers the hydroperoxide anion together with an O-centered radical. The latter then added onto the oxidized olefin, generating a cation which readily underwent nucleophilic attack by the hydroperoxide anion. This hydroperoxide species can be converted into the dioxetane intermediate through expulsion of NHS, opening up the ring-opening pathway that delivers the cleavage products. A broad substrate scope including various 1,1-disubstituted alkenes was provided, which were all well-tolerated in the reaction procedure as they were converted in moderate to excellent yields ranging from 61% to 90%. Additionally, several 1,2-disubstituted alkenes were introduced in the reaction. However, this appeared to be more challenging as the respective cleavage products were only formed between 39% and 70% yields. Das et al. also applied their reaction procedure to several complex scaffolds, all of which were underwent cleavage, delivering the products in yields ranging from 57% to 71% (**Scheme 15**). To show the application potential of their methodology, the authors also successfully performed their C=C bond cleavage under sunlight, instead of the blue LED light source. Here, they were able to convert one gram of starting material to the target eaved product in yields between 66% and 71%.



**Scheme 15** Complex olefin scope of Das' PCN-catalyzed oxidative C=C bond cleavage.

In 2020, Natarajan and co-workers performed a comparative study in which they characterized various  $BiMXO_5$  ( $M = Mg, Cd, Ni, Co, Pb, Ca$  and  $X = V, P$ ) materials using powder X-ray diffraction and optical absorption methods.<sup>74</sup> Beforehand,  $BiCdVO_5$  appeared to be promising due to its advantageous chemical stability and accessible band gap (2.45 eV).<sup>75</sup> On that account, nano and bulk  $BiCdVO_5$  were assessed in the aerobic, oxidative C=C bond cleavage reaction of styrene, which revealed the strong photocatalytic ability of the nanocatalyst in the model reaction (81%). Several other olefins were submitted to the reaction, all of them providing the respective target cleavage products in yields ranging between 76% and 89%. The reactivity of the catalyst towards the aerobic oxidation of benzyl alcohols to benzaldehydes was also assessed, revealing the catalyst's potency as the majority of the substrates provided the oxidation product in yields between 84% and 95%.

Another example of an inorganic photocatalyst was used in a contribution by the Li group, who demonstrated the potential of chalcogenide  $ZnIn_2S_4$  in the photocatalytic oxidative cleavage of C=C bonds in olefins under visible light.<sup>76</sup> Their work was inspired by the disulfide-mediated C=C bond cleavage developed by Noël and Wang, where the cleavage of S-S bonds generated reactive thiyl radicals that could reversibly add onto olefins and resulted in their activation towards oxygen capture and subsequent cycloaddition to provide a dioxetane intermediate.<sup>61</sup> On that account, Li chose benzyl mercaptane as an additive as a precursor for the thiyl radical. Since this thiol appeared to be crucial for their reaction, as no product was obtained when it was absent, the authors performed an electron paramagnetic resonance (EPR) spin-trap experiment which confirmed the generation of the thiyl radical at the valence band of the semiconductor. In a limited scope of 7 substrates, the robustness of the reaction was shown as all the olefins provided the cleavage product between 65% and 81%. Additionally, upon adding an alcohol under an air atmosphere, 7 olefins were converted to their respective acetal in yields ranging between 56% and 81%.

In 2021, Niu and co-workers aimed to design a reaction procedure for the oxidative C=C bond cleavage without the need for an initiator such as disulfides,<sup>62</sup> thiols,<sup>76</sup> or NHS.<sup>72, 77</sup> They were convinced that hydroxyl radicals ( $\cdot OH$ ) could be used, which are traditionally generated via the electron transfer from adsorbed hydroxyl ions or water to the holes of the semiconductor.<sup>78</sup> However, in this reaction, Niu proposed that the hydroxyl radicals were obtained via HAT from water to  $O_2^{\cdot-}$ , the latter being generated at the conduction band of the tubular carbon nitride (TCN) catalyst. At the valence band, on the other hand, the olefin substrate was supposedly oxidized to deliver a radical cation. Subsequently, when a hydroxyl radical adds onto this intermediate, a cationic intermediate is formed which can undergo a nucleophilic attack from  $\cdot OH$ . By releasing water, a dioxetane intermediate was formed, which underwent a cleavage process to yield the oxidized products. This mechanism was preferred over a traditional cycloaddition between the radical cation of the substrate and  $O_2^{\cdot-}$ , since isotope-labelling experiments have shown that the oxygen atom in the reaction product stemmed from  $H_2O$ . The authors

additionally revealed with an extensive substrate scope, that after formation of the aldehyde product, further oxidative coupling with MeOH could afford methyl esters under photo-oxidative conditions.<sup>79</sup>

### C≡C bond cleavage

Currently, there aren't many reports on the visible-light-induced cleavage of C≡C bonds due to their BDE being the highest of the types of carbon-carbon bonds (C≡C BDE = 954 kJ/mol,<sup>79</sup> C=C BDE = 728 kJ/mol,<sup>80</sup> C-C BDE 618 kJ/mol)<sup>81</sup> and their tendency to be over-oxidized (**Figure 1**).<sup>82</sup> Additionally, the majority of the reports are focused on the transformation of terminal alkynes such as phenylacetylene as these are more sterically accessible than 1,2-disubstituted alkynes.

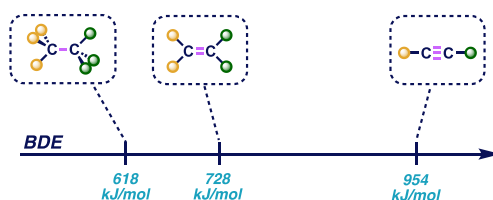


**Figure 1** Values of BDE for carbon-carbon single, double and triple bonds.

### Homogeneous catalyst

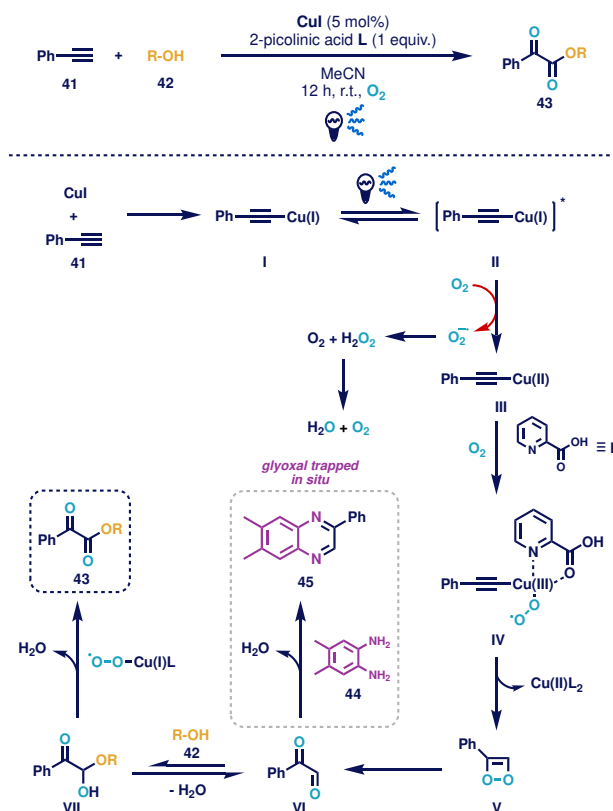
The report from Itoh in 2013 on the aerobic photo-oxidative cleavage of carbon-carbon triple bonds was the result of a follow-up study about their work on the C=C bond cleavage using CBr<sub>4</sub> as the catalyst under photoirradiation.<sup>83</sup> In that case, various olefins were converted to their respective aldehyde (or ketone) product.<sup>50</sup> In their work from 2013, however, the use of alkynes as substrates allowed for the synthesis of carboxylic acids. The presence of two intermediates, namely 2,2-dibromoacetophenone and phenylglyoxylic acid, was confirmed as the reaction product was obtained upon using both as a substrate. Based on the presence of these intermediates, the mechanism was proposed to follow either of three pathways. All three of them ended in the capture of O<sub>2</sub> by an acyl radical, after which consecutive HAT and HBr-mediated elimination of HOBr delivered the carboxylic acid product. The substrate scope proved that primarily substituted phenylacetylenes were tolerated, however also some 1,2-disubstituted alkynes were converted to their respective carboxylic acid in moderate to high yields. When introducing heterocyclic or aliphatic alkynes into the reaction, yield did not exceed 34%.

Another report by Lee on the oxidative C≡C bond cleavage was already briefly mentioned with the synthesis of azulene-1-yl ketones via oxidative cleavage of C=C bonds in *N*-sulfonyl enamides.<sup>56</sup> Here, the *N*-sulfonyl enamide substrates could also be prepared *in situ* via a tandem Cu-catalyzed [3+2] cycloaddition, Rh-catalyzed arylation, photooxygenation, and ring-opening reaction in one pot under air and sunlight. For this, the authors relied on a known procedure from literature, in which a wide range of *N*-tosyl enamides were prepared from the reaction of azulene with triazoles.<sup>84</sup> After phenylacetylene reacted with *N*-tosyl azide in the presence of the copper catalyst, a rhodium complex and azulene were added to the reaction mixture. After a treatment with Cs<sub>2</sub>CO<sub>3</sub>, 1-benzoyl azulene was obtained in 66% yield in one pot. Surprisingly, no alkyne substrate scope was performed.

In 2016, Hwang and co-workers designed a copper(I)-catalyzed oxidative coupling of 2-aminopyridine with terminal alkynes via visible-light-promoted C≡C bond cleavage.<sup>85</sup> The copper(I)phenylacetylide complex that was obtained through oxidative addition of the alkyne to the copper(I) center, could be excited by visible light, allowing for a SET to oxygen gas to generate O<sub>2</sub><sup>•-</sup> and copper(II) phenylacetylide.<sup>86</sup> After nucleophilic addition of 2-aminopyridine, a Cu(III) complex was formed which underwent consecutive reductive elimination and reaction with oxygen to afford a pyridine ketoamide intermediate and regeneration of CuCl.<sup>87</sup> Free 2-aminopyridine also coordinated with Cu(I), which yielded a superoxo/-peroxo complex upon excitation and subsequent electron transfer to O<sub>2</sub>.<sup>88</sup> This complex then abstracted a hydrogen atom from the pyridine ketoamide, generating an *N*-centered radical. Radical-assisted CO-elimination and recombination of radicals led to the formation of the pyridyl benzamide product.

Continuing their work on copper(I)-mediated C≡C bond cleavage, Hwang and co-workers designed a novel procedure for the synthesis of  $\alpha$ -keto esters via the photo-oxidative C≡C bond cleavage of terminal alkenes (**Scheme 16**).<sup>89</sup> Since it was shown that copper(I) phenylacetylide can generate copper(II) phenylacetylide and O<sub>2</sub><sup>•-</sup> under visible-light irradiation, the authors were convinced that both species could execute the controlled oxidation of the C≡C bond in alkynes.<sup>90</sup>

During their optimization, they observed that among CuCl, CuBr, and CuI, only the latter provided the product in acceptable yields. As the ligand **L**, 1 equivalent of 2-picolinic acid was found to be optimal. Removal of O<sub>2</sub> or light led to no product formation, confirming their crucial role in the reaction mechanism. After oxidative addition of phenylacetylene **41** to the copper center, excitation under visible light allowed for a SET to generate copper(II) phenylacetylene **III** and O<sub>2</sub><sup>•-</sup>. Next, coordination of 2-picolinic acid to the copper center and subsequent reaction with O<sub>2</sub> delivered the copper(III)-superoxo complex **IV**, which allowed for a rearrangement to provide intermediate **V** upon elimination of Cu<sup>II</sup>(pic)<sub>2</sub>. Through O-O bond cleavage of intermediate **V**, 2-oxo-2-phenylacetaldehyde **VI** was formed, which was converted to the hemiacetal **VII** by a nucleophilic attack of an alcohol **42**. The α-keto ester product **43** was then finally obtained through a copper-catalyzed aerobic oxidation.<sup>91</sup> The authors provided a broad and diverse alcohol and terminal alkyne scope, both of which demonstrated the robustness of their procedure as all but 4 substrates out of 43 were converted to their respective products in yields of 70% or higher. Additionally, the synthesis of 2-phenyl quinoxaline **45**, an FLT3 inhibitor, was carried out by trapping the phenylglyoxal **VI** intermediate *in situ* using a commercially available 1,2-phenylenediamine **44**.



**Scheme 16** Mechanism of Hwang's copper-catalyzed C≡C bond cleavage of phenylacetylene.

In 2020, the Sharada group were able to synthesize oxamates via the visible-light-mediated photocatalytic oxidative cleavage of alkynes.<sup>92</sup> In this report, disubstituted, electron-deficient alkynes, instead of the conventional terminal alkynes, underwent hydroamination with various aniline-derivatives as the coupling partner. After this activation mechanism, the hydroamination product would oxidatively quench the excited photocatalyst to yield the rose bengal radical anion and an N-centered radical cation. The reduced photocatalyst could then initiate a SET to *t*-butyl hydroperoxide (TBHP) to generate the reactive tertiary butoxide radical and hydroxide anion, hereby closing the rose bengal catalytic cycle. On the other hand, the radical cation generated earlier underwent consecutive radical addition by a tertiary butyl peroxide radical and nucleophilic attack by a hydroxide anion to deliver intermediate X. After an intramolecular cyclization by releasing *t*-BuOH, a dioxetane intermediate was formed which provided the oxamate product after fragmentation. The substrate scope revealed that a broad range of anilines were tolerated, unlike the alkynes where deviation from the methyl or ethyl ester scaffolds resulted in no product formation.

### Heterogeneous catalyst

A procedure designed by Ji and co-workers in 2020 made use of porous g-C<sub>3</sub>N<sub>4</sub> as a photocatalyst for the aerobic oxidative cleavage of C≡C bonds in alkynes to form aldehydes in one pot.<sup>80</sup> They had already performed a similar reaction four years earlier, where they, in a similar fashion, reacted diazonium salts with terminal alkynes using eosin Y to generate α-chloro and α-alkoxy aryl ketones.<sup>93</sup> In both cases, the diazonium salt acted as a precursor to generate aryl radicals that could undergo a radical addition to the alkyne, generating an alkenyl radical. This species would then react with O<sub>2</sub><sup>•-</sup> that was generated by SET reduction of the photocatalyst, forming a radical dioxetane intermediate that readily cleaved to deliver an aryl aldehyde and acyl radical. The latter could then be quenched via HAT, yielding the second aldehyde product. However, in their first report of 2016, the formation of the dioxetane radical intermediate was

---

considered a side reaction, and O-O bond cleavage of the peroxy radical obtained after the addition of O<sub>2</sub><sup>•-</sup> to the alkenyl radical eventually delivered the α-substituted aryl ketone the authors aimed for.

## Conclusion

Overall, we've provided a broad overview on the recent developments for the cleavage of carbon-carbon single, double, and triple bonds where light was crucial for the reaction. As we've demonstrated, the scope of this type of reactions is still rather limited, whereas only activated single bonds can be cleaved. Regarding double and triple bonds, the majority of the reports involve terminal alkenes and alkynes, currently restricting the application potential of these procedures in industry. However, looking at the growth that this field has seen in such a brief period, we're convinced that during the following years, major developments in the selective photocatalytic C-C bond cleavage will contribute to the facile and rapid synthesis of pharmaceuticals and other complex organic scaffolds, with photoredox catalysis playing a crucial role. We believe that this application window can be achieved due to the increasing development of new heterogeneous catalysts and their advantageous contributions in organic synthesis. For example, single atom photocatalysts (SAPC's) have only recently been investigated for their potential to generate ROS such as H<sub>2</sub>O<sub>2</sub>.<sup>94</sup> Due to the unsaturated coordination of the active metal centers, these catalysts exhibit remarkable activity while maintaining the recyclability of heterogeneous catalysts. We are convinced that the future of photocatalytic C-C bond cleavages will be determined by the development of novel, powerful, and selective heterogeneous catalysts which will open up the possibility for these reactions to be applied in fine chemical synthesis and the pharmaceutical industry.

## Funding Information

We thank Francqui Foundation (Francqui lecturer award of SD) for their generous support.

## Acknowledgment

Special thanks to Dr. Rakesh Maiti and Mr. Robin Cauwenbergh for their kind help during the preparation of this manuscript.

## Conflict of Interest

There are no conflicts to declare.

## References



- (1) a) Crabtree, R. H., Dion, R. P., Gibboni, D. J., McGrath, D. V., Holt, E. M., *J. Am. Chem. Soc.* **2002**, *108*, 7222; b) Terao, Y., Wakui, H., Satoh, T., Miura, M., Nomura, M., *J. Am. Chem. Soc.* **2001**, *123*, 10407; c) Kondo, T., Nakamura, A., Okada, T., Suzuki, N., Wada, K., Mitsudo, T.-a., *J. Am. Chem. Soc.* **2000**, *122*, 6319; d) Tokunaga, M., Aoyama, H., Shirogane, Y., Obora, Y., Tsuji, Y., *Catal. Today* **2006**, *117*, 138.
  - (2) Rybtchinski, B., Milstein, D., *Angew. Chem. Int. Ed.* **1999**, *38*, 870.
  - (3) Simoes, J. A. M., Beauchamp, J. L., *Chem. Rev.* **2002**, *90*, 629.
  - (4) Nolan, S. P., Hoff, C. D., Stoutland, P. O., Newman, L. J., Buchanan, J. M., Bergman, R. G., Yang, G. K., Peters, K. S., *J. Am. Chem. Soc.* **2002**, *109*, 3143.
  - (5) Adams, D. M., Chatt, J., Guy, R. G., Sheppard, N., *J. Chem. Soc.* **1961**, *0*, 738.
  - (6) Chen, F., Wang, T., Jiao, N., *Chem. Rev.* **2014**, *114*, 8613.
  - (7) a) Wu, X., Zhu, C., *Chin. J. Chem.* **2018**, *37*, 171; b) Sivaguru, P., Wang, Z., Zanoni, G., Bi, X., *Chem. Soc. Rev.* **2019**, *48*, 2615.
  - (8) Jin, J., MacMillan, D. W., *Nature* **2015**, *525*, 87; b) Marzo, L., Pagire, S. K., Reiser, O., König, B., *Angew. Chem. Int. Ed.* **2018**, *57*, 10034; c) Neumeier, M., Chakraborty, U., Schaarschmidt, D., de la Pena O'Shea, V., Perez-Ruiz, R., von Wangelin, A. J., *Angew. Chem. Int. Ed.* **2020**, *59*, 13473.
  - (9) a) Cauwenbergh, R., Das, S., *Green Chem.* **2021**, *23*, 2553; b) Crisenza, G. E. M., Melchiorre, *Nat. Commun.* **2020**, *11*; c) Twilton, J., Le, C. C., Zhang, P., Shaw, H., Evans, R. W. MacMillan, D. W. C., *Nat. Rev. Chem.* **2017**, *1*, 0052.
  - (10) Cai, S., Zhao, X., Wang, X., Liu, Q., Li, Z., Wang, D. Z., *Angew. Chem. Int. Ed.* **2012**, *51*, 8050.
  - (11) Yu, X. Y., Zhao, Q. Q., Chen, J., Chen, J. R., Xiao, W. J., *Angew. Chem. Int. Ed.* **2018**, *57*, 15505.
  - (12) Lu, B., Cheng, Y., Chen, L.-Y., Chen, J.-R., Xiao, W.-J., *ACS Catal.* **2019**, *9*, 8159.
  - (13) Fan, X., Lei, T., Chen, B., Tung, C. H., Wu, L. Z., *Org. Lett.* **2019**, *21*, 4153.
  - (14) Pratt, D. A., Blake, J. A., Mulder, P., Walton, J. C., Korth, H. G., Ingold, K. U., *J. Am. Chem. Soc.* **2004**, *126*, 10667.
  - (15) Xia, P. J., Ye, Z. P., Hu, Y. Z., Song, D., Xiang, H. Y., Chen, X. Q., Yang, H., *Org. Lett.* **2019**, *21*, 2658.
  - (16) Ladouceur, S., Fortin, D., Zysman-Colman, E., *Inorg. Chem.* **2011**, *50*, 11514.
  - (17) Stache, E. E., Ertel, A. B., Tomislav, R., Doyle, A. G., *ACS Catal.* **2018**, *8*, 11134.
  - (18) Sun, H., Yang, C., Gao, F., Li, Z., Xia, W., *Org. Lett.* **2013**, *15*, 624.
  - (19) Gazi, S., Hung Ng, W. K., Ganguly, R., Putra Moeljadi, A. M., Hirao, H., Soo, H. S., *Chem. Sci.* **2015**, *6*, 7130.
  - (20) a) Nichols, J. M., Bishop, L. M., Bergman, R. G., Ellman, J. A., *J. Am. Chem. Soc.* **2010**, *132*, 12554; b) Nguyen, J. D., Matsuura, B. S., Stephenson, C. R., *J. Am. Chem. Soc.* **2014**, *136*, 1218.
  - (21) Gazi, S., Đokić, M., Moeljadi, A. M. P., Ganguly, R., Hirao, H., Soo, H. S., *ACS Catal.* **2017**, *7*, 4682.
  - (22) Wang, Y., Liu, Y., He, J., Zhang, Y., *Sci. Bull.* **2019**, *64*, 1658.
  - (23) Guo, J. J., Hu, A., Chen, Y., Sun, J., Tang, H., Zuo, Z., *Angew. Chem. Int. Ed.* **2016**, *55*, 15319.
  - (24) Yayla, H. G., Wang, H., Tarantino, K. T., Orbe, H. S., Knowles, R. R., *J. Am. Chem. Soc.* **2016**, *138*, 10794.
  - (25) Ota, E., Wang, H., Frye, N. L., Knowles, R. R., *J. Am. Chem. Soc.* **2019**, *141*, 1457.
  - (26) Wang, D., Mao, J., Zhu, C., *Chem. Sci.* **2018**, *9*, 5805.
  - (27) Jia, K., Zhang, F., Huang, H., Chen, Y., *J. Am. Chem. Soc.* **2016**, *138*, 1514.
  - (28) Zhao, K., Yamashita, K., Carpenter, J. E., Sherwood, T. C., Ewing, W. R., Cheng, P. T. W., Knowles, R. R., *J. Am. Chem. Soc.* **2019**, *141*, 8752.
  - (29) Shi, J. L., Wang, Z., Zhang, R., Wang, Wang, Y., J., *Chem. Eur. J.* **2019**, *25*, 8992.
-



- 
- (30) Chen, Y., Du, J., Zuo, Z., *Chem* **2020**, *6*, 266.
- (31) Nguyen, S. T., McLoughlin, E. A., Cox, J. H., Fors, B. P., Knowles, R. R., *J. Am. Chem. Soc.* **2021**, *143*, 12268.
- (32) Du, J., Yang, X., Wang, X., An, Q., He, X., Pan, H., Zuo, Z., *Angew. Chem. Int. Ed.* **2021**, *60*, 5370.
- (33) Li, K. K., Lu, Y. J., Song, X. H., She, Z. G., Wu, X. W., An L. K., Ye, C. X., Lin, Y. C., *Bioorg. Med. Chem. Lett.* **2010**, *20*, 3326.
- (34) Liu, Q., Zhang, J., Zhang, L., Mo, F., *Tetrahedron* **2021**, *80*, 131867.
- (35) a) Doucet, H., *Eur. J. Org. Chem.* **2008**, *2008*, 2013; b) Jana, R., Pathak, T. P., Sigman, M. S., *Chem. Rev.* **2011**, *111*, 1417.
- (36) Vinodgopal, K., Wynkoop, D. E., Kamat, P. V., *Environ. Sci. Technol.* **1996**, *30*, 1660.
- (37) a) Jia, X., Han, Q., Zheng, M., Bi, H., *Appl. Surf. Sci.* **2019**, *489*, 409; b) Fouda, A., Salem, S. S., Wassel, A. R., Hamza, M. F., Shaheen, T. I., *Heliyon* **2020**, *6*, e04896; c) Yulizar, Y., Eprasatya, A., Apriandanu, D. O. B., Yunarti, R. T., *Vacuum* **2021**, *183*, 109821; d) Du, P., Bueno-López, A., Verbaas, M., Almeida, A. R., Makkee, M., Moulijn, J. A., Mul, G., *J. Catal.* **2008**, *260*, 75.
- (38) Jin, X., Li, C., Xu, C., Guan, D., Cheruvathur, A., Wang, Y., Xu, J., Wei, D., Xiang, H., Niemantsverdriet, J. W., Li, Y., Guo, Q., Ma, Z., Su, R., Yang, X., *J. Catal.* **2017**, *354*, 37.
- (39) Li, C., Wang, X., Cheruvathur, A., Shen, Y., Xiang, H., Li, Y., Niemantsverdriet, J. W., Su, R., *J. Catal.* **2018**, *365*, 313.
- (40) Liu, H., Li, H., Lu, J., Zeng, S., Wang, M., Luo, N., Xu, S., Wang, F., *ACS Catal.* **2018**, *8*, 4761.
- (41) a) Ballini, R., Bosica, G., Fiorini, D., Palmieri, A., Petrini, M., *Chem. Rev.* **2005**, *105*, 933; b) Muniz, K., Hovellmann, C. H., Streuff, J., *J. Am. Chem. Soc.* **2008**, *130*, 763.
- (42) a) Reymond, S., Cossy, J., *Chem. Rev.* **2008**, *108*, 5359; b) Kawasaki, M., Yamamoto, H., *J. Am. Chem. Soc.* **2006**, *128*, 16482.
- (43) a) Deshmukh, P. H., Blechert, S., *Dalton Trans.* **2007**, 2479; b) McReynolds, M. D., Dougherty, J. M., Hanson, P. R., *Chem. Rev.* **2004**, *104*, 2239.
- (44) a) Bell, S., Wustenberg, B., Kaiser, S., Menges, F., Netscher, T., Pfaltz, A., *Science* **2006**, *311*, 642; b) Scharnagl, F. K., Hertrich, M. F., Ferretti, F., Kreyenschulte, C., Lund, H., Jackstell, R., Beller, M., *Sci. Adv.* **2018**, *4*, eaau1248.
- (45) a) Temkin, O. N., *Kinet. Catal.* **2020**, *61*, 663; b) Yu, W., Zhao, Z., *Org. Lett.* **2019**, *21*, 7726.
- (46) a) Matyjaszewski, K., Sigwalt, P., *Polym. Int.* **1994**, *35*, 1; b) Matyjaszewski, K., *Makromol. Chem.-M. Symp.* **1992**, *54*, 51.
- (47) Criegee, R., *Angew. Chem. Int. Ed.* **1975**, *14*, 745.
- (48) Pappo, R., Allen, J. D., Lemieux, R., Johnson, W., *J. Org. Chem.* **2003**, *21*, 478.
- (49) a) Schilling, W., Zhang, Y., Sahoo, P. K., Sarkar, S. K., Sivaraman, G., Roesky, H. W., Das, S., *Green Chem.* **2021**, *23*, 379; b) Zhang, Y., Schilling, W., Riemer, D., Das, S., *Nat. Protoc.* **2020**, *15*, 822; c) Schilling, W., Zhang, Y., Riemer, D., Das, S., *Chem. Eur. J.* **2020**, *26*, 390; d) Zhang, Y., Schilling, W., Das, S., *ChemSusChem* **2019**, *12*, 2898; e) Kollmann, J., Zhang, Y., Schilling, W., Zhang T., Riemer, D., Das, S., *Green Chem.* **2019**, *21*, 1916; f) Zhang, Y., Riemer, D., Schilling, W., Kollmann, J., Das, S., *ACS Catal.* **2018**, *8*, 6659; g) Schilling, W., Riemer, D., Zhang, Y., Hatami, N., Das, S., *ACS Catal.* **2018**, *8*, 5425.
- (50) Hirashima, S.-i., Kudo, Y., Nobuta, T., Tada, N., Itoh, A., *Tetrahedron Lett.* **2009**, *50*, 4328.
- (51) Itoh, A., Kodama, T., Masaki, Y., Inagaki, S., *Synlett* **2002**, *2002*, 0522.
- (52) Itoh, A., Fujiya, A., Kariya, A., Nobuta, T., Tada, N., Miura, T., *Synlett* **2014**, *25*, 884.
- (53) Murthy, R. S., Bio, M., You, Y., *Tetrahedron Lett.* **2009**, *50*, 1041.
- (54) Singh, A. K., Chawla, R., Yadav, L. D. S., *Tetrahedron Lett.* **2015**, *56*, 653.
- (55) Wang, D., Li, J., Cai, S., Chen, J., Zhao, Y., *Synlett* **2014**, *25*, 1626.
- (56) Park, S., Jeon, W. H., Yong, W. S., Lee, P. H., *Org. Lett.* **2015**, *17*.
- (57) Vilsmeier, A., Haack, A., *Chem. Ber.* **1927**, *60*, 119.
- (58) Friedel, C., Crafts, J. M., *J. Chem. Soc.* **1877**, *32*, 725.
- (59) a) Gers, C. F., Rosellen, J., Merkul, E., Muller, T. J., *Beilstein J. Org. Chem.* **2011**, *7*, 1173; b) Sigrist, R., Hansen, H.-J., *Helv. Chim. Acta* **2010**, *93*, 1545.
- (60) a) Ando, W., Saiki, T., Migita, T., *J. Am. Chem. Soc.* **2002**, *97*, 5028; b) Eriksen, J., Foote, C. S., Parker, T. L., *J. Am. Chem. Soc.* **2002**, *99*, 6455.
- (61) Cao, S., Zhong, S., Xin, L., Wan, J.-P., Wen, C., *ChemCatChem* **2015**, *7*, 1478.
- (62) Deng, Y., Wei, X. J., Wang, H., Sun, Y., Noel, T., Wang, X., *Angew. Chem. Int. Ed.* **2017**, *56*, 832.
- (63) a) Ito, O., Matsuda, M., *J. Am. Chem. Soc.* **2002**, *101*, 1815; b) Ito, O., Matsuda, M., *J. Am. Chem. Soc.* **2002**, *104*, 1701.
- (64) Denes, F., Pichowicz, M., Povie, G., Renaud, P., *Chem. Rev.* **2014**, *114*, 2587.
- (65) Kharasch, M. S., Nudenberg, W., Mantell, G. J., *J. Org. Chem.* **2002**, *16*, 524.
- (66) Yu, Q., Zhang, Y., Wan, J.-P., *Green Chem.* **2019**, *21*, 3436.
- (67) Ghogare, A. A., Greer, A., *Chem. Rev.* **2016**, *116*, 9994.
- (68) Wan, J. P., Gao, Y., Wei, L., *Chem. Asian J.* **2016**, *11*, 2092.
- (69) Shiraiishi, Y., Teshima, Y., Hirai, T., *J. Phys. Chem. B* **2006**, *110*, 6257.
- (70) a) Fox, M. A., Chen, C. C., *J. Am. Chem. Soc.* **2002**, *103*, 6757; b) Kanno, T., Oguchi, T., Sakuragi, H., Tokumaru, K., *Tetrahedron Lett.* **1980**, *21*, 467; c) Kuwahara, Y., Magatani, Y., Yamashita, H., *Rapid Commun. Photoscience* **2015**, *4*, 19.
- (71) Ayed, C., Caire da Silva, L., Wang, D., Zhang, K. A. I., *J. Mater. Chem. A* **2018**, *6*, 22145.
- (72) Zhang, Y., Hatami, N., Lange, N., Ronge, E., Schilling, W., Jooss, C., Das, S., *Green Chem.* **2020**, *22*, 4516.
- (73) Su, F., Mathew, S. C., Lipner, G., Fu, X., Antonietti, M., Blechert, S., Wang, X., *J. Am. Chem. Soc.* **2010**, *132*, 16299.
- (74) Bhim, A., Sasmal, S., Gopalakrishnan, J., Natarajan, S., *Chem. Asian J.* **2020**, *15*, 3104.
- (75) a) Olchowka, J., Colmont, M., Kabbour, H., Mentré, O., *J. Alloys Compd.* **2017**, *709*, 373; b) Radosavljevic, I., Howard, J. A. K., Sleight, A. W., *Int. J. Inorg. Mater.* **2000**, *2*, 543.
- (76) Wang, X., Li, Y., Li, Z., *Catal. Sci. Technol.* **2021**, *11*, 1000.
- (77) Wang, H., Jia, R., Hong, M., Miao, H., Ni, B., Niu, T., *Green Chem.* **2021**, *23*, 6591.
- (78) a) Yang, B., Chen, Y., Shi, J., *Chem. Rev.* **2019**, *119*, 4881; b) Teong, S. P., Li, X., Zhang, Y., *Green Chem.* **2019**, *21*, 5753.
- (79) Zhang, L., Yi, H., Wang, J., Lei, A., *Green Chem.* **2016**, *18*, 5122.
- (80) Wang, J., Ni, B., Niu, T., Ji, F., *Catal. Sci. Technol.* **2020**, *10*, 8458.
- (81) Luo, Y. R., *Comprehensive Handbook of Chemical Bond Energies*, CRC Press, **2007**.
- (82) a) Pritzkow, W., Rao, T. S. S., *J. Prakt. Chem.* **1985**, *327*, 887; b) Kolle, S., Batra, S., *Org. Biomol. Chem.* **2016**, *14*, 11048.
- (83) Itoh, A., Yamaguchi, T., Nobuta, T., Kudo, Y., Hirashima, S.-i., N. Tada, Miura, T., *Synlett* **2013**, *24*, 607.
- (84) Park, S., Yong, W. S., Kim, S., Lee, P. H., *Org. Lett.* **2014**, *16*, 4468.
- (85) Ragupathi, A., Sagadevan, A., Lin, C. C., Hwu, J. R., Hwang, K. C., *Chem. Commun. (Camb.)* **2016**, *52*, 11756.
- (86) Majek, M., von Wangelin, A. J., *Angew. Chem. Int. Ed.* **2013**, *52*, 5919.
- (87) Li, J., Neuville, L., *Org. Lett.* **2013**, *15*, 1752.
-

- 
- (88) Allen, S. E., Walvoord, R. R., Padilla-Salinas, R., Kozlowski, M. C., *Chem. Rev.* **2013**, *113*, 6234.  
(89) Das, D. K., Pampana, V. K. K., Hwang, K. C., *Chem. Sci.* **2018**, *9*, 7318.  
(90) a) Sagadevan, A., Lyu, P.-C., Hwang, K. C., *Green Chem.* **2016**, *18*, 4526; b) Sagadevan, A., Charpe, V. P., Ragupathi, A., Hwang, K. C., *J. Am. Chem. Soc.* **2017**, *139*, 2896.  
(91) Das, O., Paine, T. K., *Dalton Trans.* **2012**, *41*, 11476.  
(92) Katta, N., Ojha, M., Murugan, A., Arepally, S., Sharada, D. S., *RSC Adv.* **2020**, *10*, 12599.  
(93) Niu, T. F., Jiang, D. Y., Li, S. Y., Ni, B. Q., Wang, L., *Chem. Commun. (Camb.)* **2016**, *52*, 13105.  
(94) Chu, C., Zhu, Q., Pan, Z., Gupta, S., Huang, D., Du, Y., Weon, S., Wu, Y., Muhich, C., Stavitski, E., Domen, K., Kim, J. H., *Proc. Natl. Acad. Sci. U. S. A.* **2020**, *117*, 6376.

## Biosketches

	<p><b>Shoubhik Das</b> studied chemistry in India, after which he completed his PhD in 2011 under Prof. Matthias Beller in Rostock, Germany. After a postdoctoral fellowship with Prof. Matthew J. Gaunt at the University of Cambridge, he worked at the École Polytechnique Fédérale de Lausanne (EPFL), Switzerland up until 2015. Then, he started as an independent research group leader at the Georg-August-Universität Göttingen, Germany after which they moved to the University of Antwerp in 2019.</p>
	<p><b>Jaro Vanderghinste</b> is currently conducting his doctoral studies in the research group of prof. Shoubhik Das at the University of Antwerp, where he finished his Bachelor's and Master's degree in 2019 and 2021, respectively.</p>